Carbohydrate Polymers 82 (2010) 100–105

Contents lists available at ScienceDirect

Carbohydrate Polymers

journal homepage: www.elsevier.com/locate/carbpol

Self-assembly immobilization of hyaluronan thiosemicarbazone on a gold surface for cell culture applications

Nobuo Tanaka, Yuka Yoshiike, Chiharu Yoshiyama, Takuya Kitaoka*

Department of Forest and Forest Products Sciences, Graduate School of Bioresource and Bioenvironmental Sciences, Kyushu University, 6-10-1 Hakozaki, Higashi-ku, Fukuoka 812-8581, Japan

ARTICLE INFO

Article history:
Received 1 March 2010
Received in revised form 2 April 2010
Accepted 13 April 2010
Available online 20 April 2010

Keywords:
Hyaluronan
Self-assembly
Immobilization
Cell culture
Biointerface

ABSTRACT

Hyaluronan (HA)-fixed layers were successfully prepared on a gold coated glass plate *via* self-assembly chemisorption of HA derivatives whose aldehydic reducing ends were selectively modified with thiosemicarbazide (TSC). Quartz crystal microbalance analysis and X-ray photoelectron spectroscopy suggested formation of the HA layers on the gold surfaces through spontaneous S–Au interaction, resulting in stability in aqueous culture medium. Biological functions of the HA layers were investigated by cell adhesion assay using mouse fibroblast cells (NIH-3T3). Cell attachment to the hydrophilic HA surface (water contact angle ≈ 11°) was far superior to cell attachment to a sugar-free, hydrophobic gold substrate (≈57°), while a spin-coated film composed of water-soluble, TSC-free HA molecules made little contribution to cell adhesion. After 48 h incubation, the NIH-3T3 cells proliferated well only on the HA layers and retained their original viability. This novel approach to surface glyco-modification with biocompatible HA is expected to have potential applications as a biofunctional scaffold for cell culture applications.

1. Introduction

Hyaluronan (HA, also called hyaluronic acid) is a linear glycosaminoglycan made up of D-glucuronic acid (GlcA) and *N*-acetyl-D-glucosamine (GlcNAc) units linked *via* alternating β-1,4 and β-1,3 glycosidic bonds. HA exists as the major component of the extracellular matrix (ECM) of all vertebrate animals, and is distributed widely *in vivo* (Fraser, Laurent, & Laurent, 1997; Schiller, Fuchs, Arnhold, & Arnold, 2003). Current advances in glycobiology have revealed that HA and related ECMs play fundamental roles in regulating various cellular processes involved in cell growth, proliferation, migration and differentiation (Bulpitt & Aeschlimann, 1999; Oerther et al., 1999). Hence, *in vitro* applications of HA have attracted increasing attention in biological, medical and pharmaceutical engineering fields (Barbucci et al., 2005).

A variety of scaffold materials for cell culture in tissue engineering applications have been recently developed, for *in vitro* control of cell adhesion and specific cellular functions (Boyan, Hummert, Dean, & Schwartz, 1996; Lim, Liu, Vogler, & Donahue, 2004; Park et al., 2003). It has become clear that cells sense and respond to various signals from biomaterial surfaces (biointerfaces), depending on their physicochemical, topographical and electrostatic properties. To understand such cell response mechanisms and to develop new biofunctional materials, many researchers have made efforts to design artificial ECMs using metals, ceramics, polymers and composites (Couet, Rajan, & Mantovani, 2007; Du et al., 2006; Jagur-Grodzinski, 2006; Lim et al., 2007; Nakanishi et al., 2006). HA-type ECMs are one of the most promising candidates, and HA-derived membranes have been prepared by chemical crosslinking and/or gelation with some additives (Oerther et al., 1999; Pasqui, Atrei, & Barbucci, 2007). Such treatments have significant influence on the chemical structure and inherent functions of HA; for that reason, there has been a strong need for another approach to fabricating water-soluble HA in a layer form for direct application in aqueous cell culture.

In our previous work cellulose, a β-1,4-linked D-glucose polymer, was successfully formed into a crystalline nanolayer *via* site-selective S-derivatization of its reducing end with thiosemicarbazide (TSC) and spontaneous chemisorption on a gold (Au) surface through covalent S–Au bonding, in aqueous *N*-methylmorpholine *N*-oxide (NMMO) solvent (Yokota, Kitaoka, Sugiyama, & Wariishi, 2007a). This cellulose self-assembled monolayer (SAM) possessed an inherent intra- and inter-molecular hydrogen bonding system, resulting in the formation of a crystalline structure with a parallel chain alignment (type I). The preparation protocol for cellulose-SAM has been subsequently applied to several water-soluble cellulose derivatives such as methylcellulose, carboxymethylcellulose and hydroxyethylcellulose (Yokota, Matsuyama, Kitaoka, & Wariishi, 2007b; Yokota, Kitaoka, & Wariishi, 2008a), and is expected to facili-

* Corresponding author. Tel.: +81 92 642 2993; fax: +81 92 642 2993.
E-mail address: tkitaoka@agr.kyushu-u.ac.jp (T. Kitaoka).

0144-8617/$ – see front matter © 2010 Elsevier Ltd. All rights reserved.
doi:10.1016/j.carbpol.2010.04.028

tate design of a broad range of functional polysaccharide-based biointerfaces.

In the present study HA-TSC was synthesized by reductive amination of the reducing end of HA with TSC, followed by self-assembly immobilization on an Au surface, in a similar manner to that reported for cellulose and its derivatives. The as-prepared HA-fixed layer was subjected to surface characterization and cell culture assay. Cell adhesion and proliferation, which are fundamental cellular responses, are discussed with regard to the relationship between the surface morphology of the HA-fixed layer and cell behavior on that substrate.

2. Experimental

2.1. Materials

HA sodium salt (molecular weight: *ca.* 3.0×10^4 g mol^{-1}) and TSC were obtained from Nagara Science Co., Ltd. and Sigma–Aldrich Corp., respectively. Micro-cover glass (diameter: 15 mm, Matsunami Glass Ind. Ltd.) was used as a flat and transparent substrate. The water used in this study was purified with a Milli-Q system (Millipore Corp.). A mouse fibroblast cell line (NIH-3T3) was provided by DS Pharma Biomedical Co., Ltd. Dulbecco's Modified Eagle's Medium (DMEM), penicillin–streptomycin, trypsin, glutamine and ethylenediaminetetraacetic acid (EDTA) were obtained from Invitrogen Corp. Fetal bovine serum (FBS) and phosphate buffered saline (PBS) solution were purchased from Biowest Co. Ltd. and Nissui Pharmaceutical Co. Ltd., respectively. Tissue culture polystyrene (TCPS) dishes and plates (24-well) were obtained from Sumitomo Bakelite Co. Ltd. Other chemicals were reagent grade and used without further purification.

2.2. Preparation of HA-fixed layers

Aqueous HA solution (1.0%, w/w) was mixed with TSC (1.0%, w/w) and sodium cyanoborohydride (1 M) at room temperature. The pH of the mixture was adjusted within the range 5–6 by adding 0.1 M hydrochloric acid. After stirring at 65 °C for 24 h, crude HA-TSC was obtained by freeze drying. The product was purified by rinsing with ethanol and centrifugation at least three times. According to a previous method (Yokota, Kitaoka, Opietnik, Rosenau, & Wariishi, 2008b), it was confirmed that as-prepared HA-TSC possessed a ring-open, amine form from the NMR result of GlcNAc-TSC as a model component; ^{13}C NMR data (D_2O, 100.40 MHz): δ 179.8 (C=S), 174.8 (C=O), none (anomeric C-1 around δ 90); 72.3–69.7 (C-3, 4, 5), 63.3 (C-6), 54.8 (C-2), 53.2 (C-1, C–CH_2–TSC), 22.8 (–$COCH_3$). A micro-cover glass washed with piranha solution was coated with Au (with thickness *ca.* 30 nm) using an ion sputtering device (VPS-020, ULVAC Inc.). The Au-coated glass plate was soaked in 0.1% (w/w) HA-TSC solution at 40 °C for 24 h, then thoroughly washed with Milli-Q water (r.t., 3 h) and methanol (r.t., 1 h). TCS-free HA was spin-coated on an Au plate, and used as control without further treatment. The site-directed TSC-derivatization and self-assembly immobilization of HA is outlined in Fig. 1.

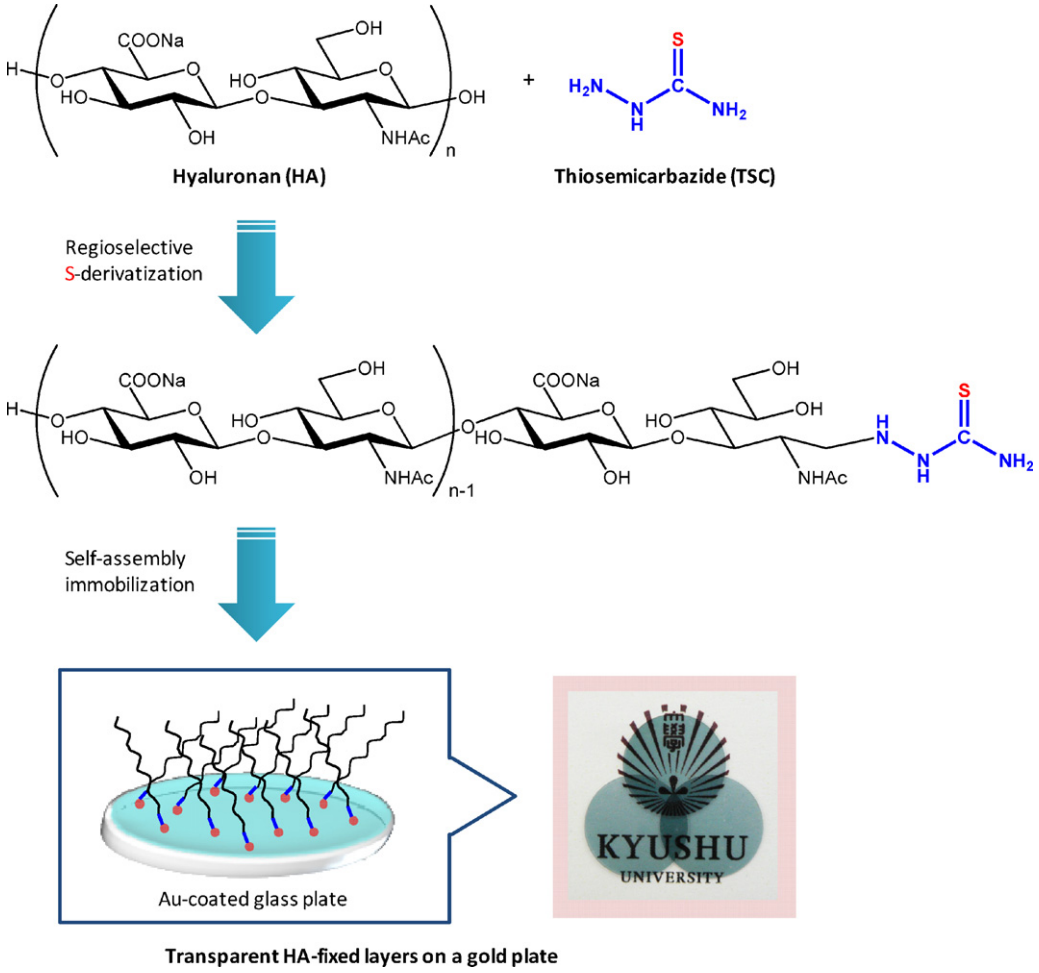

Fig. 1. Schematic illustration of the selective modification of HA with thiosemicarbazide (TSC) and the preparation of HA-fixed layers (photograph).

2.3. Characterization of HA layers

2.3.1. Quartz crystal microbalance (QCM) analysis

A QCM apparatus (AFFINIXQ, Initium Inc.) with a 27 MHz AT-cut quartz crystal (Au coated) was used to quantitatively determine the amount of HA-TSC molecules chemisorbed on the Au surface of a QCM sensor chip. The frequency changes of the sensor chip were monitored on line in a dilute aqueous solution of HA-TSC at 25 °C, stirred at 2500 rpm. The quartz probe parameters were as follows: Density, 2648 kg m^{-3}; elastic shear modulus, 2.947×10^{10} kg m^{-1} s^{-2}; surface area of Au electrode, 4.9 mm^2. In this system, 1 Hz of frequency change corresponds to 30 pg of weight variation, according to Sauerbrey's equation (Sauerbrey, 1959).

2.3.2. X-ray photoelectron spectroscopy (XPS)

Elemental analysis of the Au-coated glass plates (HA-fixed, HA-coated and HA-free) was carried out using an AXIS-HSi XPS apparatus (Shimadzu/Kratos, Co. Ltd.) equipped with a monochromatic Al Kα X-ray source (1486.6 eV). XPS analysis was performed at 15 kV voltage and 10 mA current. The analyzing chamber pressure was maintained below 0.5 μPa during the measurement. The pass energy and step width for narrow scans were set at 10 and 0.05 eV, respectively. For the survey scan, those parameters were set at 80 and 1 eV. The binding energies for all spectra were referenced to a C 1s signal (unoxidized C–C band) at 285.0 eV.

2.3.3. Contact angle (CA) measurement

The CA values of water droplets on each substrate were measured with a DropMaster 500 (Kyowa Interface Science Co. Ltd.) instrument using the sessile drop technique. A water drop (1.0 μL) was gently placed on the HA-fixed layer and other substrates at 20 °C. Digital images of the water droplets on the surfaces were periodically captured to ensure that equilibrium was reached, and simultaneously analyzed using the FACE analytical software provided with the apparatus.

2.3.4. Atomic force microscopy (AFM)

AFM imaging was performed under ambient conditions using a NanoScope IIIa (Veeco Instruments, Inc.) instrument operated in tapping mode, using single-crystal silicon cantilevers (with length 125 μm, radius of curvature 5–10 nm, spring constant 40 N m^{-1}, and resonance frequency 200–400 kHz). The AFM images were analyzed using the AFM accessory software (Version 5.12b36), and the surface roughness ('RMS') was evaluated as the root mean square deviation of the vertical profiles of horizontally averaged AFM images (1.0 μm × 1.0 μm).

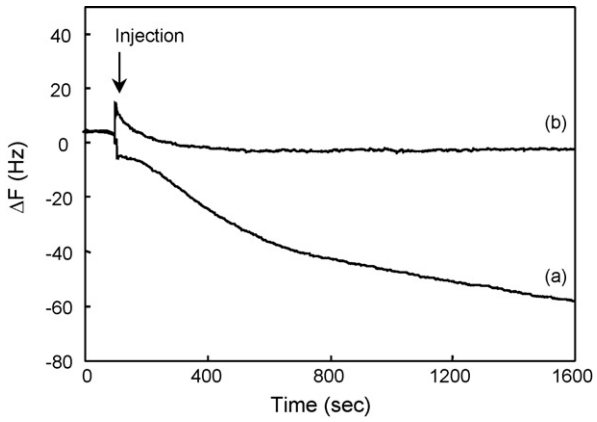

Fig. 2. QCM sensorgrams of (a) HA-TSC, and (b) TSC-free HA chemisorbed on the surface of an Au-coated sensor chip.

2.4. Cell adhesion assay

Sterilized HA-fixed layers on Au-coated glass plates were placed on 24-well TCPS plates. NIH-3T3 cell suspensions (1 mL) were seeded on each substrate (1.0×10^5 cells mL^{-1}) and incubated for 3, 6, 9, 24 and 48 h with a complete DMEM medium supplemented with 10% (v/v) FBS, 5% (v/v) penicillin–streptomycin and 2 mM glutamine in a 5% CO_2 atmosphere at 37 °C. After removal of unattached cells by twice rinsing with PBS, the residual cells adhering to the substrates were treated with trypsin–EDTA for enzymatic separation, then the detached cells were counted using a counting chamber ($n > 3$). Microscopic images were acquired with a Leica DMI 4000B (Leica Microsystems Co. Ltd.). After 48 h incubation, cell viability was assessed optically using a live/dead viability assay kit from Molecular Probes (L-3224). Live and dead cells were separately stained with 2 μM calcein AM solution (green) and 4 μM ethidium monodimmer-1 solution (red), respectively.

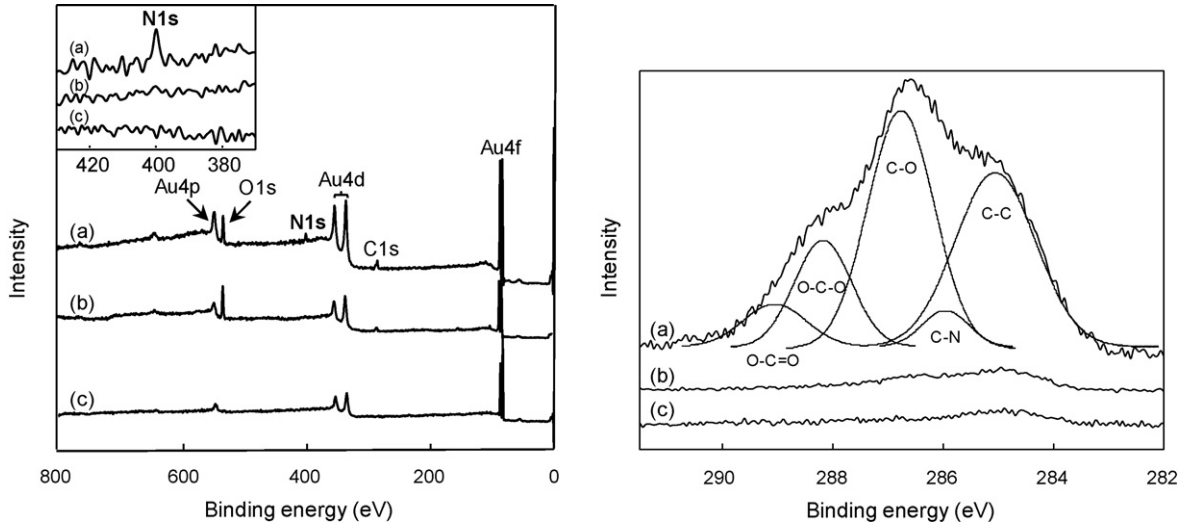

Fig. 3. XPS survey (left) and C 1s narrow scan (right) spectra of the surfaces of Au-coated glass plates treated with (a) HA-TSC, (b) TSC-free HA; (c) refers to the intact (unmodified) Au surface. The inset in the left figure shows magnified XPS spectra around the N 1s signal.

3. Results and discussion

3.1. Self-assembly immobilization of HA-TSC on a gold surface

Scaffold-molding of water-soluble HA sodium salts for cell culture requires stable, strong fixation of HA molecules on the substrate surface. In this study, self-assembly *via* S–Au chemisorption was used for the immobilization of HA-TSC. The affinity of HA-TSC for the Au matrix was estimated from the mass of HA-TSC chemisorbed on the Au surface in pure water, by using QCM which can detect mass variations of the order of picograms. Fig. 2 shows the QCM sensorgrams obtained using an Au-coated QCM sensor chip in Milli-Q water. The resonant frequency of the sensor chip was immediately decreased by the injection of HA-TSC, while negligible variation of QCM frequency was detected after injection of TSC-free HA. This indicates that HA-TSC was spontaneously chemisorbed on the Au surface *via* the formation of S–Au bonds, whereas TSC-free, unmodified HA showed only very weak interaction with the Au substrate. The surface density of HA-TSC on the Au chip was estimated as *ca.* 2.2×10^3 chains μm^{-2} from the molecular weight of HA, binding mass estimated by Sauerbrey's equation and the surface area of the QCM chip.

The elemental composition and chemical states of the surfaces of Au-coated glass plates treated with HA-TSC and TSC-free HA were determined by XPS analysis, as shown in Fig. 3. In the survey-scan spectrum for HA-TSC, a clear N 1s peak was detected at *ca.* 400 eV, suggesting successful immobilization of HA-TSC on the Au surface. For TSC-free HA no N 1s peak was found, and the XPS spectrum was almost the same as that of Au-coated glass plate. Thus physical adsorption of HA was negligible, and the TSC modification of HA reducing ends was indispensable for immobilization to the

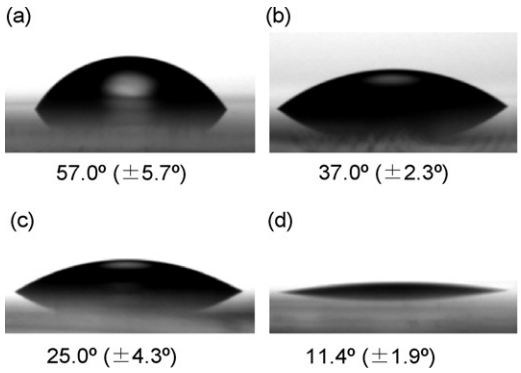

Fig. 4. Optical images and contact angles of a water droplet on each substrate. (a) Au-coated plate, (b) TSC-treated Au plate, (c) HA spin coat and (d) HA-fixed layer.

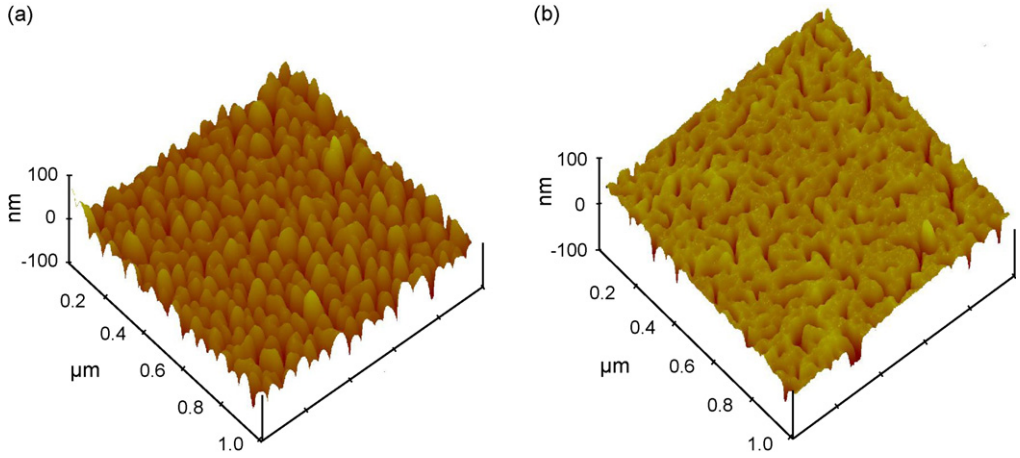

Fig. 5. AFM topographical images of (a) HA-fixed layer, and (b) intact Au-coated glass plate. The RMS values are 10.62 and 5.36 nm, respectively.

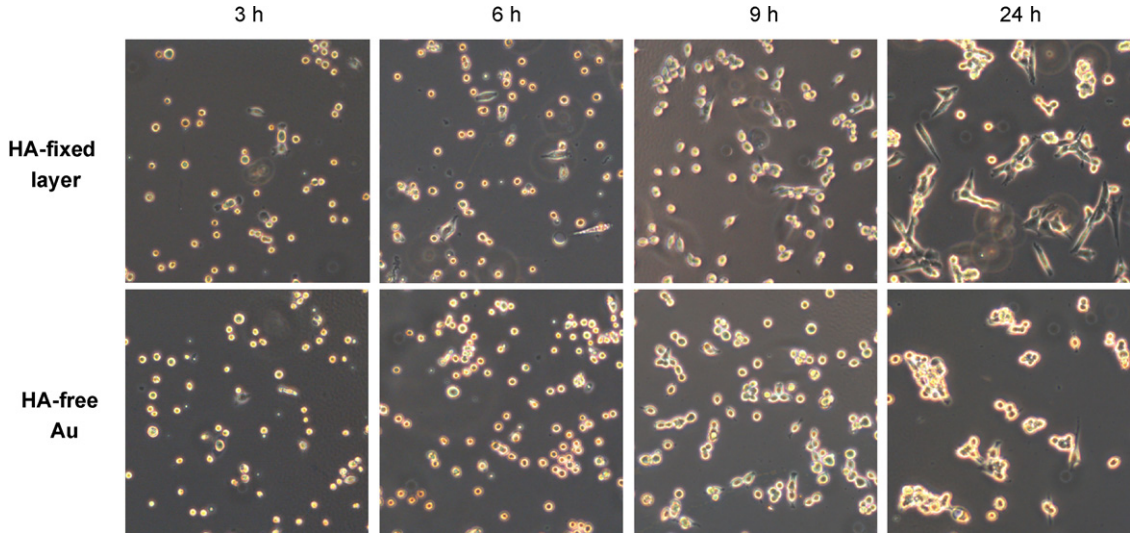

Fig. 6. Microscopic images of NIH-3T3 cells cultured on HA-fixed layer (top column), and HA-free Au (bottom column) plate. Culture time: 3–24 h. Image size: 500 μm × 500 μm.

substrate surface. The C 1s narrow spectrum of the HA-fixed layer exhibited characteristic C–C (285.0 eV), possible C–N (285.9 eV), C–O (286.7 eV), O–C–O (288.1 eV) and O–C=O (289.3 eV) signals. The C–O:O–C–O:O–C=O ratio obtained by peak deconvolution was *ca.* 8:3:1, corresponding to that of the carbon atoms of HA. The XPS profile remained unchanged even after washing (data not shown), thus stable fixation of HA molecules to the Au matrix was achieved while maintaining the chemical structure of HA in almost its original form.

3.2. Surface characteristics of HA-fixed layers

Initial cell adhesion depends strongly on the wettability of scaffold materials, which is one of the most important surface properties for cell–substrate interactions. The surface wettability of HA-fixed layers was thus investigated by CA measurement using the sessile drop technique. Fig. 4 displays the optical images and CA values of water droplets on each substrate. The immobilization of HA-TSC on the Au plate clearly enhanced the hydrophilicity (CA *ca.* 11°) due to formation of the water-soluble HA layer. The spin-coated HA layer was less hydrophilic (CA *ca.* 25°), and gradual swelling of the top layer in contact with water was observed, as shown in Fig. 4c. Thus it is suggested that HA binding *via* S–Au chemisorption was effective for forming a stable HA interface.

The AFM topographical images of the surface of each substrate are shown in Fig. 5. The intact Au-coated glass plate had a flat surface at the nanometer scale, and the immobilization of HA-TSC increased the surface roughness, with RMS values in the range 5.4–10.6. Thus, both molecular hydrophilicity and roughness factor (Wenzel's effect) must influence the higher wettability, as shown in Fig. 4d. In the case of spin-coated HA film, there was a lack of uniformity on a broad scale, and it was difficult to capture clear AFM images (data not shown). It is apparent that the self-assembly immobilization approach had the advantage of formation of flat, homogeneous HA layers.

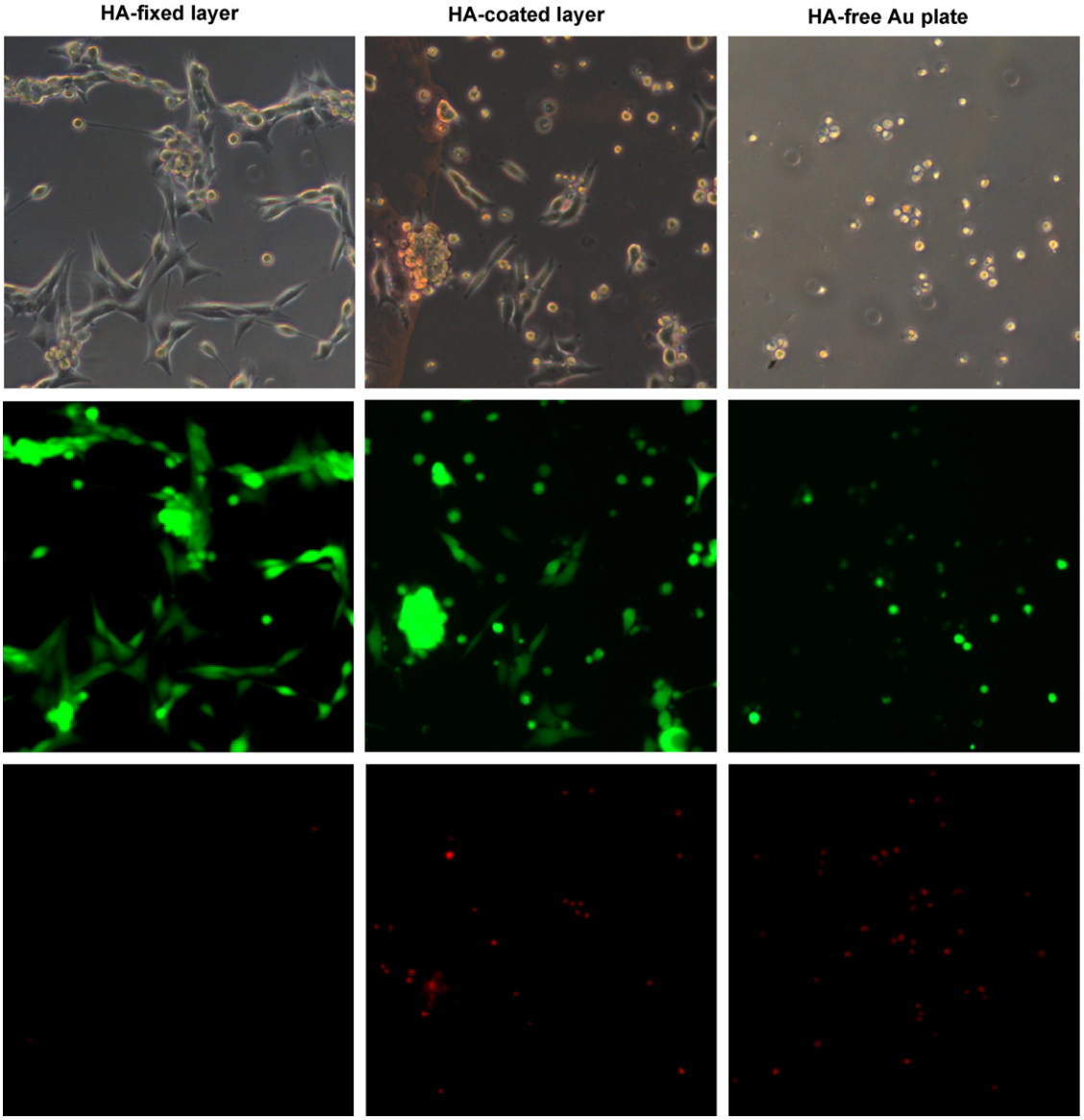

Fig. 7. Microscopic and fluorescent images of NIH-3T3 cells cultured on HA-fixed layer (left column), HA-coated Au (center column) and HA-free Au (right column) plates. Culture time: 48 h. Top: Phase-contrast micrographs. Middle and bottom: Fluorescence micrographs of live (green) and dead (red) cells. Image size: 500 μm × 500 μm. (For interpretation of the references to color in this figure legend, the reader is referred to the web version of the article.)

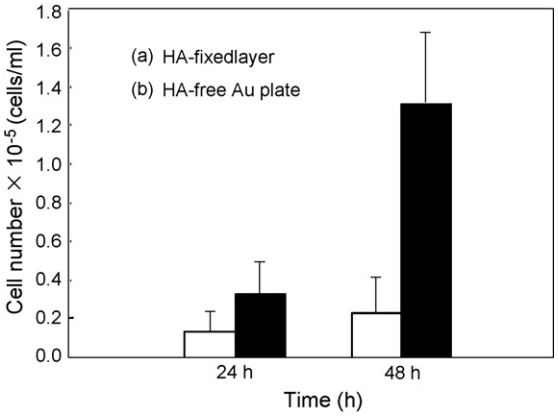

Fig. 8. Cell growth behavior of (a) HA-fixed layer, and (b) HA-free Au plate, for 24 and 48 h incubation periods.

3.3. Cell culture behavior on HA-fixed layers

Cell adhesion/proliferation assay was carried out to elucidate biofunctional characteristics of HA-fixed layers. Fig. 6 shows optical images of NIH-3T3 cells incubated on HA-fixed, HA-coated and HA-free Au substrates for 3–24 h. Both Au and HA layers were sufficiently thin to be transparent (light blue) as shown in Fig. 1, and allowed direct monitoring of cell growth over time. In the case of HA-fixed layers, good initial cell adhesion was observed, and most cells had a flat morphology and spread laterally. On the other hand, most of the cells on HA-free Au plate aggregated, resulting in poor cell attachment. Fig. 7 compares optical and fluorescent images of NIH-3T3 cells on each substrate after 48 h incubation. Vital cells adhering well to the substrate surface were observed on the HA-fixed layer (left column), while there were few living cells in normal shapes found on HA-coated (center column) and HA-free (right column) Au plates. The HA scaffold on the HA-coated substrate was gradually broken down in an aqueous culture medium, and the fibroblast cells presumably had less affinity for the Au plate. Such cells eventually floated on the culture medium, and were presumed to be dead (most of the floating cells were removed with serum to prepare the fluorescence micrograph). These results agreed with the fluorescent microscopic images, resulting in the clear difference of detection of only live cells on HA-fixed layers and many dead cells on HA-coated and HA-free Au plates.

Fig. 8 shows the growth behavior of NIH-3T3 cells adhering to an HA-fixed layer and an HA-free Au plate. The fixed HA molecules possessed significant ability to enhance cell adhesion and proliferation, resulting in the original viability of NIH-3T3 cells on the HA layer, as shown in Fig. 7. The great difference in the cell behavior strongly suggested the advantages of HA-type scaffold for practical applications. The facile preparation through self-assembly immobilization of terminal S-modified HA on the Au surface, and resulting high performance for cell culture, are expected to assist in the design of diverse physiological functions of *in vivo* polysaccharides for *in vitro* biological applications.

4. Conclusion

Reducing end S-termination of HA molecules as the major component of ECM *in vivo* with TSC was carried out and as-prepared HA-TSCs were successfully immobilized on an Au-coated glass plate *via* self-assembly chemisorption. The biological properties of HA-fixed interface were investigated by cell adhesion assay, and mouse fibroblast cell NIH-3T3 adhered to the HA-fixed substrate, proliferated well and retained the original cell viability, whereas simple HA-coated surface and intact Au substrates possessed poor biofunctionality. Thus, this approach demonstrates the biofunctionality of HA molecules in a layer state for cell culture applications.

Acknowledgment

This research was supported by a Grant-in-Aid for Young Scientists (S: 21678002) from the Ministry of Education, Culture, Sports, Science and Technology, Japan (T.K.).

References

Barbucci, R., Magnani, A., Chiumiento, A., Pasqui, D., Cangioli, I., & Lamponi, S. (2005). Fibroblast cell behavior on bound and adsorbed fibronectin onto hyaluronan and sulfated hyaluronan substrates. *Biomacromolecules*, *6*, 638–645.

Boyan, B. D., Hummert, T. W., Dean, D. D., & Schwartz, Z. (1996). Role of material surfaces in regulating bone and cartilage cell response. *Biomaterials*, *17*, 137–146.

Bulpitt, P., & Aeschlimann, D. (1999). New strategy for chemical modification of hyaluronic acid: Preparation of functionalized derivatives and their use in the formation of novel biocompatible hydrogels. *Journal of Biomedical Materials Research*, *47*, 152–169.

Couet, F., Rajan, N., & Mantovani, D. (2007). Macromolecular biomaterials for scaffold-based vascular tissue engineering. *Macromolecular Bioscience*, *7*, 701–718.

Du, Y., Chia, S.-M., Han, R., Chang, S., Tang, H., & Yu, H. (2006). 3D hepatocyte monolayer on hybrid RGD/galactose substratum. *Biomaterials*, *27*, 5669–5680.

Fraser, J. R., Laurent, T. C., & Laurent, U. B. (1997). Hyaluronan: Its nature, distribution, functions and turnover. *Journal of Internal Medicine*, *242*, 27–33.

Jagur-Grodzinski, J. (2006). Polymers for tissue engineering, medical devices, and regenerative medicine. Concise general review of recent studies. *Polymers for Advanced Technologies*, *17*, 395–418.

Lim, J. Y., Liu, X., Vogler, E. A., & Donahue, H. J. (2004). Systematic variation in osteoblast adhesion and phenotype with substratum surface characteristics. *Journal of Biomedical Materials Research A*, *68*, 504–512.

Lim, J. Y., Dreiss, A. D., Zhou, Z., Hansen, J. C., Siedlecki, C. A., Hengstebeck, R. W., et al. (2007). The regulation of integrin-mediated osteoblast focal adhesion and focal adhesion kinase expression by nanoscale topography. *Biomaterials*, *28*, 1787–1797.

Nakanishi, J., Kikuchi, Y., Takarada, T., Nakayama, H., Yamaguchi, K., & Maeda, M. (2006). Spatiotemporal control of cell adhesion on a self-assembled monolayer having a photocleavable protecting group. *Analytica Chimica Acta*, *578*, 100–104.

Oerther, S., Le, G. H., Payan, E., Lapicque, F., Presle, N., Hubert, P., et al. (1999). Hyaluronate-alginate gel as a novel biomaterial: Mechanical properties and formation mechanism. *Biotechnology and Bioengineering*, *63*, 206–215.

Park, I.-K., Yang, J., Jeong, H.-J., Bom, H.-S., Harada, I., Akaike, T., et al. (2003). Galactosylated chitosan as a synthetic extracellular matrix for hepatocytes attachment. *Biomaterials*, *24*, 2331–2337.

Pasqui, D., Atrei, A., & Barbucci, R. (2007). A novel strategy to obtain a hyaluronan monolayer on solid substrates. *Biomacromolecules*, *8*, 3531–3539.

Sauerbrey, G. (1959). The use of quartz crystal oscillators for weighing thin layers and for micro-weighing. *Zeitschrift fur Physik*, *155*, 206–222.

Schiller, J., Fuchs, B., Arnhold, J., & Arnold, K. (2003). Contribution of reactive oxygen species to cartilage degradation in rheumatic diseases: Molecular pathways, diagnosis and potential therapeutic strategies. *Current Medicinal Chemistry*, *10*, 2123–2145.

Yokota, S., Kitaoka, T., Sugiyama, J., & Wariishi, H. (2007a). Cellulose I nanolayers designed by self-assembly of its thiosemicarbazone on a gold substrate. *Advanced Materials*, *19*, 3368–3370.

Yokota, S., Matsuyama, K., Kitaoka, T., & Wariishi, H. (2007b). Thermally responsive wettability of self-assembled methylcellulose nanolayers. *Applied Surface Science*, *253*, 5149–5154.

Yokota, S., Kitaoka, T., & Wariishi, H. (2008a). Biofunctionality of self-assembled nanolayers composed of cellulosic polymers. *Carbohydrate Polymers*, *74*, 666–672.

Yokota, S., Kitaoka, T., Opietnik, M., Rosenau, T., & Wariishi, H. (2008b). Synthesis of gold nanoparticles for in situ conjugation with structural carbohydrates. *Angewandte Chemie International Edition*, *47*, 9866–9869.